

## Improved Kelson-Garvey mass relations for proton-rich nuclei

Junlong Tian,<sup>1,\*</sup> Ning Wang,<sup>2</sup> Cheng Li,<sup>1,2</sup> and Jingjing Li<sup>1</sup>

<sup>1</sup>*School of Physics and Electrical Engineering, Anyang Normal University, Anyang 455000, People's Republic of China*

<sup>2</sup>*Department of Physics, Guangxi Normal University, Guilin 541004, People's Republic of China*

(Received 18 October 2012; published 11 January 2013)

The improved Kelson-Garvey (ImKG) mass relations are proposed from the mass differences of mirror nuclei. The masses of 31 measured proton-rich nuclei with  $7 \leq A \leq 41$  and  $-5 \leq (N - Z) \leq -3$  can be remarkably well reproduced by using the proposed relations, with a root-mean-square deviation of 0.398 MeV, which is much smaller than the results of Kelson-Garvey (0.502 MeV) and isobar-mirror mass relations (0.647 MeV). This is because many more masses of participating nuclei are involved in the ImKG mass relations for predicting the masses of unknown proton-rich nuclei. The masses for 144 unknown proton-rich nuclei with  $6 \leq A \leq 74$  are predicted by using the ImKG mass relations. The one- and two-proton separation energies for these proton-rich nuclei and the diproton emission are investigated simultaneously.

DOI: [10.1103/PhysRevC.87.014313](https://doi.org/10.1103/PhysRevC.87.014313)

PACS number(s): 21.10.Dr, 21.10.Sf, 21.30.Fe, 23.90.+w

### I. INTRODUCTION

Nuclear mass (or binding energy), which reflects directly the sum effect of the strong, weak, and electromagnetic interactions among the participating nucleons, plays a vital role in nuclear physics and astrophysics. In nuclear physics, nuclear masses are of great importance for the development of nuclear structure models and the prediction of exotic decay modes and new symmetries. With the help of radioactive beam facilities, a variety of nuclei near or beyond the proton drip line have been produced, including the heaviest and most proton-rich doubly magic nucleus  $^{48}\text{Ni}$  [1]. In astrophysics, the investigation of nucleosynthesis and energy generation in the rapid proton capture (rp) process [2,3] and  $\nu p$  process [4] depends on the masses of proton-rich nuclei. The rp-process path approaches the proton drip line for heavy nuclei. The proton-separation energy  $S_p$  is of particular interest to the  $\nu p$  process as it is a process that could resolve the longstanding underproduction of light p nuclei. Accurate predictions for the masses of proton drip-line nuclei is therefore urgently required for understanding the rp process and  $\nu p$  process [5,6].

Available nuclear mass formulas include some global and local formulas. Some global nuclear mass models have been successfully established, such as the Duflo-Zuker model [7], the finite range droplet model (FRDM) [8], the Skyrme Hartree-Fock-Bogoliubov theory [9–11], and the Weizsäcker-Skyrme (WS) mass model [12–14]. For drip-line nuclei, the differences between the calculated masses from these different models are quite large. The local mass formulas are generally based on algebraic or systematic approaches. They predict the masses of unknown nuclei from the masses of known neighboring nuclei, such as the Audi-Wapstra systematics [15–17], the Garvey-Kelson mass relations [18–25], and the mass relations based on the residual proton-neutron interactions [26–29]. The main difficulty of the available local mass formulas is that the model errors rapidly increase for nuclei far from the measured nuclei. On the other hand, the concept of symmetry in physics is a very powerful tool for understanding

the behavior of nature. The isospin symmetry discovered by Heisenberg plays an important role in nuclear physics. In the absence of Coulomb interactions between the protons, a perfectly charge-symmetric and charge-independent nuclear force would result in the binding energies of mirror nuclei being identical. It is therefore necessary to establish some mass relations for description of the masses of proton-drip line nuclei according to the mirror effect coming from the isospin symmetry in nuclear physics.

In this work, we attempt to establish some mass relations for the description of the mass of proton-rich nuclei. The paper is organized as follows. In Sec. II, the improved Kelson-Garvey (ImKG) mass relations are proposed from the mass differences of mirror nuclei including the higher-order mirror nuclei and ordinary mirror nuclei near the  $N = Z$  line. In Sec. III, the masses of 144 proton-rich nuclei are calculated with the proposed method. The one- and two-proton separation energies of nuclei, and the diproton emission of nuclei are investigated simultaneously. Finally, a summary is given in Sec. IV.

### II. IMPROVED KELSON-GARVEY MASS RELATIONS

#### A. Kelson-Garvey mass relations

A simple and successful procedure has been introduced by Kelson and Garvey (KG) [30,31]. It is a mass relation that connects masses of higher-order mirror nuclei with ordinary mirror nuclei near the  $N = Z$  line,

$$B(A, -Y) - B(A, Y) = \sum_{j=-Y}^{+Y-1} [B(A + j, Y = -1) - B(A + j, Y = 1)], \quad (1)$$

where  $B(A, Y)$  is the binding energy of a nucleus, which can be expressed as a function of mass number  $A$  and isotopic number  $Y = N - Z$ , and  $j$  is to be increased by a step of 2.

The binding energy differences between the most proton-rich and most neutron-rich members of an isospin multiplet can hence be estimated from known binding energy differences between  $Y = 1$  mirror nuclei. A heuristic proof of this relation can again be obtained from an independent particle picture

\*tianjunlong@gmail.com

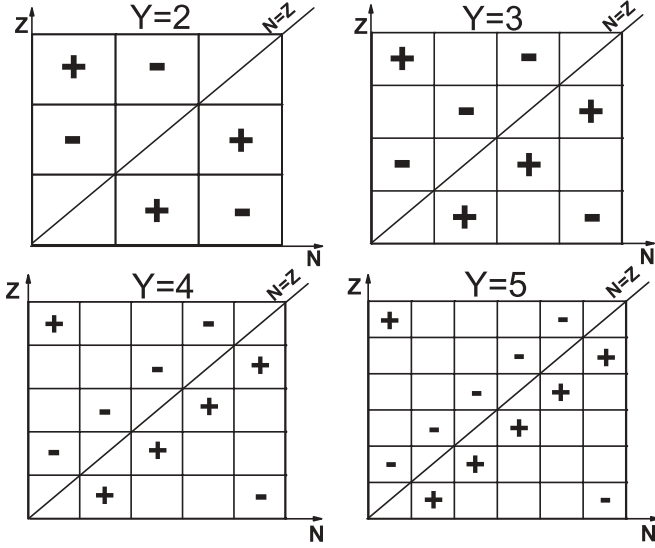


FIG. 1. Schematic representation of the charge-symmetric Kelson-Garvey mass relation Eq. (1) for four examples,  $Y = 2 - 5$ . The boxes represent nuclei from the nuclidic chart, and the plus and minus signs indicate that the respective mass values have to be added or subtracted.

with fourfold degenerate Hartree-Fock or Nilsson-like single-particle levels. Figure 1 shows the schematic representation of the charge-symmetric KG mass relation Eq. (1) for four examples with  $Y = 2 - 5$ . The boxes represent nuclei from the nuclidic chart, and the plus and minus signs indicate that the respective mass values have to be added or subtracted. The binding energy differences for the  $Y = 1$  mirror nuclei up to  $A = 75$  were taken from the experimental mass table given in Ref. [32].

### B. Improved Kelson-Garvey (ImKG) mass relations

According to the KG mass relation of Eq. (1), the binding energy difference between a pair of mirror nuclei can be written as

$$B(A, -2) - B(A, 2) \approx B(A - 1, -1) - B(A - 1, 1) + B(A + 1, -1) - B(A + 1, 1), \quad (2)$$

for  $Y = 2$  case, and

$$B(A, -3) - B(A, 3) \approx B(A - 2, -1) - B(A - 2, 1) + B(A, -1) - B(A, 1) + B(A + 2, -1) - B(A + 2, 1), \quad (3)$$

for  $Y = 3$  case.

Applying Eq. (2), we rewrite Eq. (3) as follows (see Fig. 2)

$$B(A, -3) - B(A, 3) \approx B(A - 1, -2) - B(A - 1, 2) + B(A + 2, -1) - B(A + 2, 1), \quad (4)$$

or

$$B(A, -3) - B(A, 3) \approx B(A - 2, -1) - B(A - 2, 1) + B(A + 1, -2) - B(A + 1, 2). \quad (5)$$

Through the summation of Eqs. (3)–(5), we can obtain the following expression as an improved Kelson-Garvey mass relation (see  $Y = 3$  case in Fig. 3)

$$3[B(A, -3) - B(A, 3)] \approx 2B(A - 2, -1) - 2B(A - 2, 1) + B(A, -1) - B(A, 1) + 2B(A + 2, -1) - 2B(A + 2, 1) + B(A - 1, -2) - B(A - 1, 2) + B(A + 1, -2) - B(A + 1, 2), \quad (6)$$

or

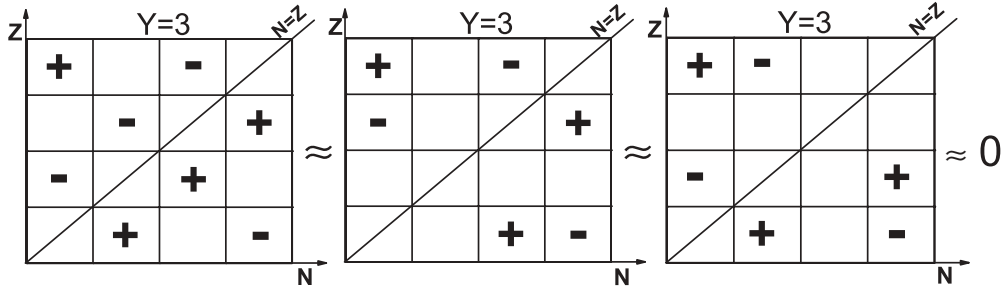
$$3B(A, -3) - B(A + 1, -2) - 2B(A + 2, -1) + 0B(A + 3, 0) - B(A - 1, -2) - B(A, -1) + 0B(A + 1, 0) + 2B(A + 2, 1) - 2B(A - 2, -1) + 0B(A - 1, 0) + B(A, 1) + B(A + 1, 2) - 0B(A - 3, 0) + 2B(A - 2, 1) + B(A - 1, 2) - 3B(A, 3) \approx 0. \quad (7)$$

In the same fashion, one can predict the binding energy of unknown proton-rich nucleus  $B(A, -4)$  by expression (see  $Y = 4$  case in Fig. 3)

$$7[B(A, -4) - B(A, 4)] \approx 4[B(A - 3, -1) - B(A - 3, 1)] + 2[B(A - 1, -1) - B(A - 1, 1)] + 2[B(A + 1, -1) - B(A + 1, 1)] + 4[B(A + 3, -1) - B(A + 3, 1)] + 2[B(A - 2, -2) - B(A - 2, 2)] + [B(A, -2) - B(A, 2)] + 2[B(A + 2, -2) - B(A + 2, 2)] + [B(A - 1, -3) - B(A - 1, 3)] + [B(A + 1, -3) - B(A + 1, 3)]. \quad (8)$$

Following a format similar to Eqs. (6) and (8), the following general relationship is obtained as the improved Kelson-Garvey mass relation:

$$(2^{Y-1} - 1)[B(A, -Y) - B(A, Y)] \approx \sum_{i=1}^{(Y-1)} \left\{ 2^{Y-i-1} [B(A - (Y - i), -i) - B(A - (Y - i), i)] + 2^{Y-i-2} \sum_{j=-(Y-i-2)}^{(Y-i-2)} [B(A + j, -i) - B(A + j, i)] + 2^{Y-i-1} [B(A + (Y - i), -i) - B(A + (Y - i), i)] \right\}, \quad (9)$$


 FIG. 2. Schematic representation of the ImKG relation Eqs. (3)–(5) for  $Y = 3$  cases.

where  $Y = 2, 3, 4, \dots$ ;  $i = 1, 2, 3, \dots, (Y - 1)$ , and  $(Y - i - 2) \geq 0$  otherwise the term  $2^{Y-i-2} \sum_{j=-(Y-i-2)}^{(Y-i-2)} [B(A + j, -i) - B(A + j, i)]$  is canceled;  $j = -(Y - i - 2), -(Y - i - 2) + 2, \dots, (Y - i - 2)$  is to be increased by step of 2.

### C. Isobar-mirror (IM) mass relations

Isobar-mirror mass relations are deduced based on three assumptions as follows: (i) The difference between the binding energies of mirror nuclei is only due to the Coulomb interaction. It is known that in the absence of Coulomb interactions between the protons, a perfectly charge-symmetric and charge-independent nuclear force would result in the binding energies of mirror nuclei being identical [33–35].

|            |            |            |           |           |           |            |            |             |            |            |            |            |            |            |            |            |
|------------|------------|------------|-----------|-----------|-----------|------------|------------|-------------|------------|------------|------------|------------|------------|------------|------------|------------|
| $Y=3$      |            |            |           | $Y=4$     |           |            |            |             |            |            |            |            |            |            |            |            |
| <b>+3</b>  | -1         | -2         | 0         | <b>+7</b> | -1        | -2         | -4         | 0           |            |            |            |            |            |            |            |            |
| -1         | -1         | 0          | <b>+2</b> | -1        | -1        | -2         | 0          | <b>+4</b>   |            |            |            |            |            |            |            |            |
| -2         | 0          | <b>+1</b>  | <b>+1</b> | -2        | -2        | 0          | <b>+2</b>  | <b>+2</b>   |            |            |            |            |            |            |            |            |
| 0          | <b>+2</b>  | <b>+1</b>  | -3        | -4        | 0         | <b>+2</b>  | <b>+1</b>  | <b>+1</b>   |            |            |            |            |            |            |            |            |
|            |            |            |           | 0         | <b>+4</b> | <b>+2</b>  | <b>+1</b>  | -7          |            |            |            |            |            |            |            |            |
| $Y=5$      |            |            |           | $Y=6$     |           |            |            |             |            |            |            |            |            |            |            |            |
| <b>+15</b> | -1         | -2         | -4        | -8        | 0         | <b>+31</b> | -1         | -2          | -4         | -8         | -16        | 0          |            |            |            |            |
| -1         | -1         | -2         | -4        | 0         | <b>+8</b> | -1         | -1         | -2          | -4         | -8         | 0          | <b>+16</b> |            |            |            |            |
| -2         | -2         | -4         | 0         | <b>+4</b> | <b>+4</b> | -2         | -2         | -4          | -8         | 0          | <b>+8</b>  | <b>+8</b>  |            |            |            |            |
| -4         | -4         | 0          | <b>+4</b> | <b>+2</b> | <b>+2</b> | -4         | -4         | -8          | 0          | <b>+8</b>  | <b>+4</b>  | <b>+4</b>  |            |            |            |            |
| -8         | 0          | <b>+4</b>  | <b>+2</b> | <b>+1</b> | <b>+1</b> | -8         | -8         | 0           | <b>+8</b>  | <b>+4</b>  | <b>+2</b>  | <b>+2</b>  |            |            |            |            |
| 0          | <b>+8</b>  | <b>+4</b>  | <b>+2</b> | <b>+1</b> | -15       | -16        | 0          | <b>+8</b>   | <b>+4</b>  | <b>+2</b>  | <b>+1</b>  | <b>+1</b>  |            |            |            |            |
|            |            |            |           |           |           | 0          | <b>+16</b> | <b>+8</b>   | <b>+4</b>  | <b>+2</b>  | <b>+1</b>  | -31        |            |            |            |            |
| $Y=7$      |            |            |           | $Y=8$     |           |            |            |             |            |            |            |            |            |            |            |            |
| <b>+63</b> | -1         | -2         | -4        | -8        | -16       | -32        | 0          | <b>+127</b> | -1         | -2         | -4         | -8         | -16        | -32        | -64        | 0          |
| -1         | -1         | -2         | -4        | -8        | -16       | 0          | <b>+32</b> | -1          | -1         | -2         | -4         | -8         | -16        | -32        | 0          | <b>+64</b> |
| -2         | -2         | -4         | -8        | -16       | 0         | <b>+16</b> | <b>+16</b> | -2          | -2         | -4         | -8         | -16        | -32        | 0          | <b>+32</b> | <b>+32</b> |
| -4         | -4         | -8         | -16       | 0         | <b>+8</b> | <b>+8</b>  | -4         | -4          | -8         | -16        | -32        | 0          | <b>+16</b> | <b>+16</b> |            |            |
| -8         | -8         | -16        | 0         | <b>+4</b> | <b>+4</b> | -8         | -8         | -16         | -32        | 0          | <b>+8</b>  | <b>+8</b>  | <b>+8</b>  |            |            |            |
| -16        | -16        | 0          | <b>+2</b> | <b>+2</b> | -16       | -16        | -32        | 0           | <b>+4</b>  | <b>+4</b>  | <b>+4</b>  | <b>+4</b>  |            |            |            |            |
| -32        | 0          | <b>+8</b>  | <b>+4</b> | <b>+2</b> | <b>+1</b> | <b>+1</b>  | -32        | -32         | 0          | <b>+2</b>  | <b>+2</b>  | <b>+2</b>  | <b>+2</b>  |            |            |            |
| 0          | <b>+32</b> | <b>+16</b> | <b>+8</b> | <b>+4</b> | <b>+2</b> | <b>+1</b>  | -63        | -64         | 0          | <b>+16</b> | <b>+8</b>  | <b>+4</b>  | <b>+2</b>  | <b>+1</b>  | <b>+1</b>  |            |
|            |            |            |           |           |           |            |            | 0           | <b>+64</b> | <b>+32</b> | <b>+16</b> | <b>+8</b>  | <b>+4</b>  | <b>+2</b>  | <b>+1</b>  | -127       |

 FIG. 3. (Color online) Schematic representation of the improved Kelson-Garvey mass relations given by Eq. (9) for 6 examples with  $Y = 3 - 8$ .

(ii) The Coulomb energy difference between a pair of mirror nuclei is proportional to  $Y$ , the same as the assumption used in Ref. [33],

$$\Delta B = E_C(A, -Y) - E_C(A, Y) = b(A, Y, i)Y, \quad (10)$$

in which the label  $i$  represents the microscopic corrections connected to the nuclear force, which are neglected. (iii) The coefficient of proportionality, which indeed depends on  $A$ , may be considered as independent of  $Y$  for a given  $A$ . In Refs. [33, 36], it was found that the  $b$  coefficients are roughly constant (see Tables 3–7 in Ref. [36]) for a given  $A$ , and Ormand obtained an empirical formula  $b = 0.710A^{2/3} - 0.946$  MeV by fitting to 116 experimental data with an rms deviation of 102 keV [33].

In the following calculation by using isobar-mirror mass relations, one does not need to know the exact value of  $b$  coefficients. The binding energies difference for a pair odd- $A$  mirror nuclei with different  $Y = 1, 3, 5, \dots$  reads

$$\Delta B(Y = 1) = B(A, 1) - B(A, -1) = b, \quad (11)$$

$$\Delta B(Y = 3) = B(A, 3) - B(A, -3) = 3b, \quad (12)$$

$$\Delta B(Y = 5) = B(A, 5) - B(A, -5) = 5b, \quad (13)$$

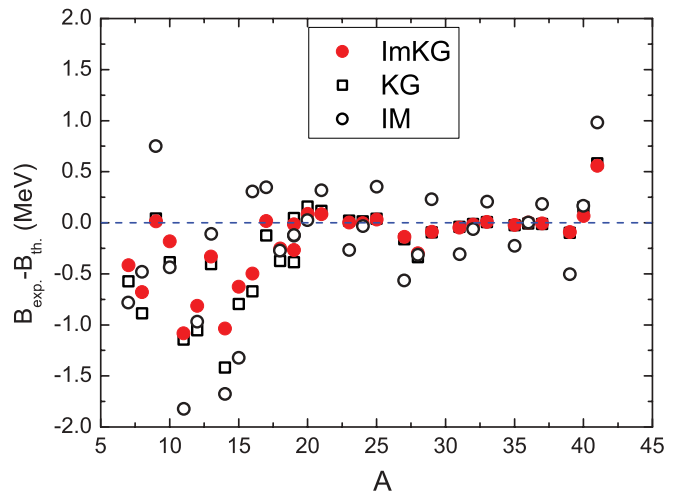


FIG. 4. (Color online) Difference between the experimental binding energies and predictions for 31 measured proton-rich nuclei with ImKG approach (solid circles), KG [31] (open squares), and IM (open circles), respectively.

TABLE I. Predicted binding energy ( $B_{\text{ImKG}}$ ), mass excess ( $M_{\text{ImKG}}$ ), and separation energies for one-proton ( $S_p$ ) and two-proton ( $S_{2p}$ ) with the ImKG mass relations for 144 proton-rich nuclei (column 1) with  $55 \leq A \leq 74$  are given in columns 3, 4, 7, and 8, respectively (in MeV). The estimated uncertainties are given in parentheses in keV. The isotopic number  $Y = N - Z$  is listed in column 2. Columns 5 and 6 list the neutron-rich analog and the measured mass excess ( $M_{\text{exp}}^{\text{analog}}$ ) with its associated error in parentheses in keV.

| ${}^A Z$           | $Y$ | $B_{\text{ImKG}}$<br>MeV (keV) | $M_{\text{ImKG}}$<br>MeV (keV) | ${}^A Z_{\text{analog}}$ | $M_{\text{exp}}^{\text{analog}}$<br>MeV (keV) | $S_p$<br>MeV (keV) | $S_{2p}$<br>MeV (keV) |
|--------------------|-----|--------------------------------|--------------------------------|--------------------------|---|--------------------|-----------------------|
| ${}^{52}\text{Co}$ | -2  | 432.983(15)                    | -34.396(15)                    | ${}^{52}\text{Mn}$       | -50.707(2)                                    | 1.466(21)          | 6.348(15)             |
| ${}^{56}\text{Cu}$ | -2  | 453.218(1)                     | -38.571(1)                     | ${}^{56}\text{Co}$       | -56.040(1)                                    | 0.526(1)           | 5.141(1)              |
| ${}^{60}\text{Ga}$ | -2  | 499.975(55)                    | -39.947(55)                    | ${}^{60}\text{Cu}$       | -58.345(2)                                    | 0.023(66)          | 2.860(55)             |
| ${}^{62}\text{Ge}$ | -2  | 517.675(66)                    | -42.287(66)                    | ${}^{62}\text{Zn}$       | -61.167(1)                                    | 2.489(107)         | 2.693(66)             |
| ${}^{64}\text{As}$ | -2  | 530.412(92)                    | -39.664(92)                    | ${}^{64}\text{Ga}$       | -58.834(1)                                    | 0.034(114)         | 2.258(92)             |
| ${}^{66}\text{Se}$ | -2  | 548.166(108)                   | -42.058(108)                   | ${}^{66}\text{Ge}$       | -61.607(2)                                    | 2.412(128)         | 2.322(108)            |
| ${}^{68}\text{Br}$ | -2  | 560.507(125)                   | -39.038(125)                   | ${}^{68}\text{As}$       | -58.895(2)                                    | -0.251(179)        | 1.589(125)            |
| ${}^{70}\text{Kr}$ | -2  | 578.734(166)                   | -41.904(166)                   | ${}^{70}\text{Se}$       | -61.930(2)                                    | 2.722(181)         | 2.294(166)            |
| ${}^{72}\text{Rb}$ | -2  | 590.613(163)                   | -38.422(163)                   | ${}^{72}\text{Br}$       | -59.067(7)                                    | -0.614(163)        | 1.577(163)            |
| ${}^{74}\text{Sr}$ | -2  | 608.812(242)                   | -41.262(242)                   | ${}^{74}\text{Kr}$       | -62.332(2)                                    | 2.474(242)         | 1.901(242)            |
| ${}^5\text{Be}$    | -3  | 3.129(120)                     | 34.097(120)                    | ${}^5\text{H}$           | 32.892(89)                                    | -1.759(165)        | -4.589(120)           |
| ${}^{43}\text{V}$  | -3  | 347.063(42)                    | -17.990(42)                    | ${}^{43}\text{Ca}$       | -38.409(0.2)                                  | 0.094(43)          | 3.926(42)             |
| ${}^{45}\text{Cr}$ | -3  | 364.134(42)                    | -19.700(42)                    | ${}^{45}\text{Sc}$       | -41.070(0.6)                                  | 3.168(47)          | 4.958(43)             |
| ${}^{47}\text{Mn}$ | -3  | 382.415(43)                    | -22.621(43)                    | ${}^{47}\text{Ti}$       | -44.936(0.4)                                  | 0.358(48)          | 5.320(46)             |
| ${}^{49}\text{Fe}$ | -3  | 399.921(45)                    | -24.767(45)                    | ${}^{49}\text{V}$        | -47.961(0.9)                                  | 2.744(53)          | 4.787(47)             |
| ${}^{51}\text{Co}$ | -3  | 417.927(27)                    | -27.412(27)                    | ${}^{51}\text{Cr}$       | -51.451(0.9)                                  | 0.179(39)          | 4.376(36)             |
| ${}^{53}\text{Ni}$ | -3  | 435.544(20)                    | -29.668(20)                    | ${}^{53}\text{Mn}$       | -54.689(0.6)                                  | 2.561(25)          | 4.026(25)             |
| ${}^{55}\text{Cu}$ | -3  | 452.943(16)                    | -31.707(16)                    | ${}^{55}\text{Fe}$       | -57.481(0.5)                                  | -0.276(17)         | 3.628(17)             |
| ${}^{57}\text{Zn}$ | -3  | 469.325(16)                    | -32.730(16)                    | ${}^{57}\text{Co}$       | -59.345(0.5)                                  | 1.447(17)          | 1.973(17)             |
| ${}^6\text{B}$     | -4  | 0.360(264)                     | 44.235(264)                    | ${}^6\text{H}$           | 41.876(254)                                   | -2.769(290)        | -4.528(288)           |
| ${}^{22}\text{Al}$ | -4  | 149.429(12)                    | 17.969(12)                     | ${}^{22}\text{F}$        | 2.793(12)                                     | 0.149(13)          | 3.378(13)             |
| ${}^{26}\text{P}$  | -4  | 186.917(5)                     | 11.203(5)                      | ${}^{26}\text{Na}$       | -6.861(3.5)                                   | -0.119(6)          | 3.291(5)              |
| ${}^{30}\text{Cl}$ | -4  | 224.010(17)                    | 4.830(17)                      | ${}^{30}\text{Al}$       | -15.872(14)                                   | -0.611(17)         | 2.653(17)             |
| ${}^{34}\text{K}$  | -4  | 261.023(1)                     | -1.462(1)                      | ${}^{34}\text{P}$        | -24.549(0.8)                                  | -0.642(2)          | 2.715(2)              |
| ${}^{38}\text{Sc}$ | -4  | 294.969(4)                     | -4.687(4)                      | ${}^{38}\text{Cl}$       | -29.798(0.1)                                  | -1.155(4)          | 1.857(4)              |
| ${}^{42}\text{V}$  | -4  | 329.011(63)                    | -8.009(63)                     | ${}^{42}\text{K}$        | -35.022(0.1)                                  | -0.351(64)         | 2.071(63)             |
| ${}^{44}\text{Cr}$ | -4  | 349.911(22)                    | -13.548(22)                    | ${}^{44}\text{Ca}$       | -41.469(0.3)                                  | 2.848(48)          | 2.942(23)             |
| ${}^{46}\text{Mn}$ | -4  | 364.406(50)                    | -12.683(50)                    | ${}^{46}\text{Sc}$       | -41.760(0.6)                                  | 0.272(66)          | 3.440(54)             |
| ${}^{48}\text{Fe}$ | -4  | 385.225(29)                    | -18.142(29)                    | ${}^{48}\text{Ti}$       | -48.492(0.4)                                  | 2.810(52)          | 3.168(37)             |
| ${}^{50}\text{Co}$ | -4  | 400.188(36)                    | -17.745(36)                    | ${}^{50}\text{V}$        | -49.224(0.9)                                  | 0.267(58)          | 3.011(46)             |
| ${}^{52}\text{Ni}$ | -4  | 420.472(27)                    | -22.668(27)                    | ${}^{52}\text{Cr}$       | -55.418(0.6)                                  | 2.545(38)          | 2.725(39)             |
| ${}^{54}\text{Cu}$ | -4  | 434.930(12)                    | -21.765(12)                    | ${}^{54}\text{Mn}$       | -55.557(1.2)                                  | -0.614(24)         | 1.947(20)             |
| ${}^{56}\text{Zn}$ | -4  | 454.211(20)                    | -25.686(20)                    | ${}^{56}\text{Fe}$       | -60.606(0.5)                                  | 1.268(27)          | 0.992(21)             |
| ${}^{13}\text{F}$  | -5  | 53.666(16)                     | 43.386(16)                     | ${}^{13}\text{Be}$       | 33.208(10)                                    | -3.235(18)         | -3.425(16)            |
| ${}^{15}\text{Ne}$ | -5  | 71.613(23)                     | 41.555(23)                     | ${}^{15}\text{B}$        | 28.964(22)                                    | -1.270(33)         | -3.532(23)            |
| ${}^{17}\text{Na}$ | -5  | 93.481(23)                     | 35.346(23)                     | ${}^{17}\text{C}$        | 21.032(17)                                    | -3.561(26)         | -3.328(23)            |
| ${}^{21}\text{Al}$ | -5  | 133.304(12)                    | 26.024(12)                     | ${}^{21}\text{O}$        | 8.062(12)                                     | -1.265(13)         | 1.496(13)             |
| ${}^{23}\text{Si}$ | -5  | 151.394(100)                   | 23.294(100)                    | ${}^{23}\text{F}$        | 3.310(100)                                    | 1.965(101)         | 2.114(100)            |
| ${}^{25}\text{P}$  | -5  | 170.495(44)                    | 19.553(44)                     | ${}^{25}\text{Ne}$       | -2.060(45)                                    | -1.507(45)         | 1.770(45)             |
| ${}^{27}\text{S}$  | -5  | 187.474(13)                    | 17.934(13)                     | ${}^{27}\text{Na}$       | -5.518(4)                                     | 0.557(14)          | 0.438(13)             |
| ${}^{29}\text{Cl}$ | -5  | 206.427(17)                    | 14.341(17)                     | ${}^{29}\text{Mg}$       | -10.603(11)                                   | -2.682(20)         | -0.341(18)            |
| ${}^{31}\text{Ar}$ | -5  | 224.410(21)                    | 11.719(21)                     | ${}^{31}\text{Al}$       | -14.955(20)                                   | 0.400(28)          | -0.212(22)            |
| ${}^{33}\text{K}$  | -5  | 243.971(6)                     | 7.518(6)                       | ${}^{33}\text{Si}$       | -20.514(0.7)                                  | -2.414(10)         | 0.040(7)              |
| ${}^{35}\text{Ca}$ | -5  | 262.100(3)                     | 4.750(3)                       | ${}^{35}\text{P}$        | -24.858(2)                                    | 1.077(6)           | 0.435(4)              |
| ${}^{37}\text{Sc}$ | -5  | 278.413(4)                     | 3.797(4)                       | ${}^{37}\text{S}$        | -26.896(0.2)                                  | -2.961(4)          | -0.370(4)             |
| ${}^{39}\text{Ti}$ | -5  | 295.276(49)                    | 2.294(49)                      | ${}^{39}\text{Cl}$       | -29.800(1.7)                                  | 0.307(50)          | -0.848(50)            |
| ${}^{41}\text{V}$  | -5  | 312.882(43)                    | 0.048(43)                      | ${}^{41}\text{Ar}$       | -33.068(0.4)                                  | -1.679(68)         | 0.447(44)             |
| ${}^{43}\text{Cr}$ | -5  | 330.352(52)                    | -2.061(52)                     | ${}^{43}\text{K}$        | -36.575(0.4)                                  | 1.341(82)          | 0.990(53)             |
| ${}^{45}\text{Mn}$ | -5  | 348.837(38)                    | -5.185(38)                     | ${}^{45}\text{Ca}$       | -40.812(0.4)                                  | -1.074(44)         | 1.773(57)             |
| ${}^{47}\text{Fe}$ | -5  | 366.237(42)                    | -7.226(42)                     | ${}^{47}\text{Sc}$       | -44.337(2)                                    | 1.832(66)          | 2.103(60)             |
| ${}^{49}\text{Co}$ | -5  | 384.300(23)                    | -9.928(23)                     | ${}^{49}\text{Ti}$       | -48.563(0.4)                                  | -0.925(38)         | 1.885(49)             |
| ${}^{51}\text{Ni}$ | -5  | 401.747(36)                    | -12.014(36)                    | ${}^{51}\text{V}$        | -52.204(0.9)                                  | 1.558(51)          | 1.826(58)             |
| ${}^{53}\text{Cu}$ | -5  | 418.858(23)                    | -13.766(23)                    | ${}^{53}\text{Cr}$       | -55.286(0.6)                                  | -1.614(35)         | 0.932(35)             |

TABLE I. (Continued.)

| ${}^A Z$           | $Y$ | $B_{\text{ImKG}}$<br>MeV (keV) | $M_{\text{ImKG}}$<br>MeV (keV) | ${}^A Z_{\text{analog}}$ | $M_{\text{exp}}^{\text{analog}}$<br>MeV (keV) | $S_p$<br>MeV (keV) | $S_{2p}$<br>MeV (keV) |
|--------------------|-----|--------------------------------|--------------------------------|--------------------------|---|--------------------|-----------------------|
| ${}^{55}\text{Zn}$ | -5  | 435.227(18)                    | -14.774(18)                    | ${}^{55}\text{Mn}$       | -57.712(0.4)                                  | 0.297(22)          | -0.317(27)            |
| ${}^{16}\text{Na}$ | -6  | 67.264(30)                     | 53.272(30)                     | ${}^{16}\text{B}$        | 37.120(27)                                    | -4.427(38)         | -5.697(38)            |
| ${}^{18}\text{Mg}$ | -6  | 92.589(32)                     | 43.306(32)                     | ${}^{18}\text{C}$        | 24.920(30)                                    | -0.672(39)         | -4.233(34)            |
| ${}^{20}\text{Al}$ | -6  | 108.982(56)                    | 42.274(56)                     | ${}^{20}\text{N}$        | 21.765(56)                                    | -2.890(60)         | -2.403(60)            |
| ${}^{22}\text{Si}$ | -6  | 134.565(57)                    | 32.051(57)                     | ${}^{22}\text{O}$        | 9.282(57)                                     | 1.261(59)          | -0.004(57)            |
| ${}^{24}\text{P}$  | -6  | 149.528(72)                    | 32.448(72)                     | ${}^{24}\text{F}$        | 7.560(72)                                     | -1.866(124)        | 0.099(74)             |
| ${}^{26}\text{S}$  | -6  | 169.856(21)                    | 27.481(21)                     | ${}^{26}\text{Ne}$       | 0.479(18)                                     | -0.639(50)         | -2.146(21)            |
| ${}^{28}\text{Cl}$ | -6  | 184.650(12)                    | 28.047(12)                     | ${}^{28}\text{Na}$       | -0.988(10)                                    | -2.824(18)         | -2.267(14)            |
| ${}^{30}\text{Ar}$ | -6  | 206.034(17)                    | 22.024(17)                     | ${}^{30}\text{Mg}$       | -8.892(13)                                    | -0.394(25)         | -3.075(20)            |
| ${}^{32}\text{K}$  | -6  | 221.665(86)                    | 21.753(86)                     | ${}^{32}\text{Al}$       | -11.062(86)                                   | -2.745(89)         | -2.345(88)            |
| ${}^{34}\text{Ca}$ | -6  | 244.182(16)                    | 14.596(16)                     | ${}^{34}\text{Si}$       | -19.957(14)                                   | 0.211(17)          | -2.203(17)            |
| ${}^{36}\text{Sc}$ | -6  | 258.300(13)                    | 15.838(13)                     | ${}^{36}\text{P}$        | -20.251(13)                                   | -3.800(14)         | -2.722(13)            |
| ${}^{38}\text{Ti}$ | -6  | 278.683(27)                    | 10.816(27)                     | ${}^{38}\text{S}$        | -26.861(7)                                    | 0.270(27)          | -2.691(27)            |
| ${}^{40}\text{V}$  | -6  | 293.334(52)                    | 11.525(52)                     | ${}^{40}\text{Cl}$       | -27.558(32)                                   | -0.942(72)         | -1.635(52)            |
| ${}^{42}\text{Cr}$ | -6  | 314.025(32)                    | 6.194(32)                      | ${}^{42}\text{Ar}$       | -34.423(6)                                    | 1.143(54)          | -0.536(62)            |
| ${}^{44}\text{Mn}$ | -6  | 329.140(59)                    | 6.439(59)                      | ${}^{44}\text{K}$        | -35.782(0.4)                                  | -1.212(79)         | 0.129(87)             |
| ${}^{46}\text{Fe}$ | -6  | 350.419(30)                    | 0.522(30)                      | ${}^{46}\text{Ca}$       | -43.140(2)                                    | 1.582(48)          | 0.508(37)             |
| ${}^{48}\text{Co}$ | -6  | 365.407(38)                    | 0.893(38)                      | ${}^{48}\text{Sc}$       | -44.503(5)                                    | -0.830(57)         | 1.002(63)             |
| ${}^{50}\text{Ni}$ | -6  | 385.746(26)                    | -4.085(26)                     | ${}^{50}\text{Ti}$       | -51.431(0.4)                                  | 1.446(35)          | 0.522(39)             |
| ${}^{52}\text{Cu}$ | -6  | 399.506(33)                    | -2.484(33)                     | ${}^{52}\text{V}$        | -51.444(0.9)                                  | -2.241(49)         | -0.683(49)            |
| ${}^{54}\text{Zn}$ | -6  | 418.649(25)                    | -6.267(25)                     | ${}^{54}\text{Cr}$       | -56.934(0.6)                                  | -0.210(34)         | -1.824(37)            |
| ${}^{19}\text{Al}$ | -7  | 88.100(99)                     | 55.085(99)                     | ${}^{19}\text{C}$        | 32.414(98)                                    | -4.489(104)        | -5.161(102)           |
| ${}^{21}\text{Si}$ | -7  | 107.977(96)                    | 50.568(96)                     | ${}^{21}\text{N}$        | 25.251(95)                                    | -1.005(111)        | -3.895(98)            |
| ${}^{23}\text{P}$  | -7  | 131.610(90)                    | 42.295(90)                     | ${}^{23}\text{O}$        | 14.621(90)                                    | -2.955(107)        | -1.694(91)            |
| ${}^{25}\text{S}$  | -7  | 147.625(76)                    | 41.641(76)                     | ${}^{25}\text{F}$        | 11.364(75)                                    | -1.904(106)        | -3.769(126)           |
| ${}^{27}\text{Cl}$ | -7  | 165.005(66)                    | 39.620(66)                     | ${}^{27}\text{Ne}$       | 7.036(65)                                     | -4.851(69)         | -5.490(80)            |
| ${}^{29}\text{Ar}$ | -7  | 182.309(14)                    | 37.677(14)                     | ${}^{29}\text{Na}$       | 2.670(12)                                     | -2.341(19)         | -5.165(19)            |
| ${}^{31}\text{K}$  | -7  | 201.481(20)                    | 33.866(20)                     | ${}^{31}\text{Mg}$       | -3.190(17)                                    | -4.554(27)         | -4.947(27)            |
| ${}^{33}\text{Ca}$ | -7  | 219.808(68)                    | 30.898(68)                     | ${}^{33}\text{Al}$       | -8.437(68)                                    | -1.857(110)        | -4.602(72)            |
| ${}^{35}\text{Sc}$ | -7  | 239.393(39)                    | 26.674(39)                     | ${}^{35}\text{Si}$       | -14.360(38)                                   | -4.789(42)         | -4.579(40)            |
| ${}^{37}\text{Ti}$ | -7  | 257.350(61)                    | 24.077(61)                     | ${}^{37}\text{P}$        | -18.996(38)                                   | -0.950(62)         | -4.750(61)            |
| ${}^{39}\text{V}$  | -7  | 275.285(64)                    | 21.503(64)                     | ${}^{39}\text{S}$        | -23.162(50)                                   | -3.398(70)         | -3.129(64)            |
| ${}^{41}\text{Cr}$ | -7  | 292.871(75)                    | 19.277(75)                     | ${}^{41}\text{Cl}$       | -27.307(68)                                   | -0.463(91)         | -2.405(90)            |
| ${}^{43}\text{Mn}$ | -7  | 311.195(44)                    | 16.314(44)                     | ${}^{43}\text{Ar}$       | -32.010(5)                                    | -2.831(55)         | -1.688(62)            |
| ${}^{45}\text{Fe}$ | -7  | 329.229(55)                    | 13.640(55)                     | ${}^{45}\text{K}$        | -36.616(0.5)                                  | 0.089(81)          | -1.123(76)            |
| ${}^{47}\text{Co}$ | -7  | 348.628(26)                    | 9.601(26)                      | ${}^{47}\text{Ca}$       | -42.345(2)                                    | -1.791(40)         | -0.209(46)            |
| ${}^{49}\text{Ni}$ | -7  | 366.043(39)                    | 7.547(39)                      | ${}^{49}\text{Sc}$       | -46.560(3)                                    | 0.636(55)          | -0.194(58)            |
| ${}^{51}\text{Cu}$ | -7  | 382.566(22)                    | 6.384(22)                      | ${}^{51}\text{Ti}$       | -49.732(0.6)                                  | -3.180(34)         | -1.734(33)            |
| ${}^{53}\text{Zn}$ | -7  | 398.054(35)                    | 6.257(35)                      | ${}^{53}\text{V}$        | -51.850(3)                                    | -1.452(48)         | -3.693(50)            |
| ${}^{22}\text{P}$  | -8  | 103.574(192)                   | 62.260(192)                    | ${}^{22}\text{N}$        | 32.039(192)                                   | -4.403(215)        | -5.408(201)           |
| ${}^{24}\text{S}$  | -8  | 129.631(111)                   | 51.563(111)                    | ${}^{24}\text{O}$        | 18.500(110)                                   | -1.980(143)        | -4.934(125)           |
| ${}^{26}\text{Cl}$ | -8  | 142.028(78)                    | 54.526(78)                     | ${}^{26}\text{F}$        | 18.665(77)                                    | -5.596(109)        | -7.499(107)           |
| ${}^{28}\text{Ar}$ | -8  | 162.067(96)                    | 49.848(96)                     | ${}^{28}\text{Ne}$       | 11.292(96)                                    | -2.939(116)        | -7.790(98)            |
| ${}^{30}\text{K}$  | -8  | 177.753(24)                    | 49.522(24)                     | ${}^{30}\text{Na}$       | 8.374(23)                                     | -4.556(28)         | -6.897(28)            |
| ${}^{32}\text{Ca}$ | -8  | 199.970(21)                    | 42.666(21)                     | ${}^{32}\text{Mg}$       | -0.912(18)                                    | -1.511(30)         | -6.064(28)            |
| ${}^{34}\text{Sc}$ | -8  | 215.226(60)                    | 42.770(60)                     | ${}^{34}\text{Al}$       | -3.047(60)                                    | -4.583(92)         | -6.440(105)           |
| ${}^{36}\text{Ti}$ | -8  | 237.755(74)                    | 35.601(74)                     | ${}^{36}\text{Si}$       | -12.418(57)                                   | -1.638(84)         | -6.427(76)            |
| ${}^{38}\text{V}$  | -8  | 253.298(81)                    | 35.419(81)                     | ${}^{38}\text{P}$        | -14.643(71)                                   | -4.053(102)        | -5.003(83)            |
| ${}^{40}\text{Cr}$ | -8  | 274.841(118)                   | 29.236(118)                    | ${}^{40}\text{S}$        | -22.930(114)                                  | -0.444(134)        | -3.843(121)           |
| ${}^{42}\text{Mn}$ | -8  | 290.059(150)                   | 29.378(150)                    | ${}^{42}\text{Cl}$       | -24.913(144)                                  | -2.812(168)        | -3.275(159)           |
| ${}^{44}\text{Fe}$ | -8  | 311.112(39)                    | 23.685(39)                     | ${}^{44}\text{Ar}$       | -32.673(2)                                    | -0.082(59)         | -2.913(51)            |
| ${}^{46}\text{Co}$ | -8  | 327.032(53)                    | 23.127(53)                     | ${}^{46}\text{K}$        | -35.414(0.7)                                  | -2.198(76)         | -2.109(79)            |
| ${}^{48}\text{Ni}$ | -8  | 349.085(29)                    | 16.433(29)                     | ${}^{48}\text{Ca}$       | -44.224(2)                                    | 0.457(39)          | -1.334(42)            |
| ${}^{50}\text{Cu}$ | -8  | 362.548(40)                    | 18.331(40)                     | ${}^{50}\text{Sc}$       | -44.546(15)                                   | -3.495(56)         | -2.859(56)            |
| ${}^{52}\text{Zn}$ | -8  | 380.445(27)                    | 15.794(27)                     | ${}^{52}\text{Ti}$       | -49.469(7)                                    | -2.121(35)         | -5.301(37)            |
| ${}^{25}\text{Cl}$ | -9  | 122.489(111)                   | 65.994(111)                    | ${}^{25}\text{O}$        | 27.348(111)                                   | -7.142(157)        | -9.121(143)           |
| ${}^{27}\text{Ar}$ | -9  | 137.381(190)                   | 66.462(190)                    | ${}^{27}\text{F}$        | 24.630(190)                                   | -4.647(206)        | -10.244(205)          |

TABLE I. (Continued.)

| ${}^A Z$           | $Y$ | $B_{\text{ImKG}}$<br>MeV (keV) | $M_{\text{ImKG}}$<br>MeV (keV) | ${}^A Z_{\text{analog}}$ | $M_{\text{exp}}^{\text{analog}}$<br>MeV (keV) | $S_p$<br>MeV (keV) | $S_{2p}$<br>MeV (keV) |
|--------------------|-----|--------------------------------|--------------------------------|--------------------------|---|--------------------|-----------------------|
| ${}^{29}\text{K}$  | -9  | 156.107(100)                   | 63.097(100)                    | ${}^{29}\text{Ne}$       | 18.400(100)                                   | -5.960(139)        | -8.899(120)           |
| ${}^{31}\text{Ca}$ | -9  | 174.356(103)                   | 60.208(103)                    | ${}^{31}\text{Na}$       | 12.540(103)                                   | -3.397(106)        | -7.954(104)           |
| ${}^{33}\text{Sc}$ | -9  | 194.918(23)                    | 55.006(23)                     | ${}^{33}\text{Mg}$       | 4.947(22)                                     | -5.052(31)         | -6.562(31)            |
| ${}^{35}\text{Ti}$ | -9  | 212.704(70)                    | 52.581(70)                     | ${}^{35}\text{Al}$       | -0.220(70)                                    | -2.522(93)         | -7.105(98)            |
| ${}^{37}\text{V}$  | -9  | 232.233(92)                    | 48.413(92)                     | ${}^{37}\text{Si}$       | -6.594(83)                                    | -5.523(118)        | -7.161(100)           |
| ${}^{39}\text{Cr}$ | -9  | 251.238(87)                    | 44.768(87)                     | ${}^{39}\text{P}$        | -12.795(81)                                   | -2.060(119)        | -6.112(106)           |
| ${}^{41}\text{Mn}$ | -9  | 270.581(74)                    | 40.785(74)                     | ${}^{41}\text{S}$        | -19.089(61)                                   | -4.260(139)        | -4.704(98)            |
| ${}^{43}\text{Fe}$ | -9  | 288.809(209)                   | 37.917(209)                    | ${}^{43}\text{Cl}$       | -24.408(206)                                  | -1.250(257)        | -4.062(222)           |
| ${}^{45}\text{Co}$ | -9  | 307.214(34)                    | 34.873(34)                     | ${}^{45}\text{Ar}$       | -29.771(0.5)                                  | -3.899(52)         | -3.981(56)            |
| ${}^{47}\text{Ni}$ | -9  | 325.905(54)                    | 31.542(54)                     | ${}^{47}\text{K}$        | -35.709(2.5)                                  | -1.126(75)         | -3.324(77)            |
| ${}^{49}\text{Cu}$ | -9  | 344.679(26)                    | 28.129(26)                     | ${}^{49}\text{Ca}$       | -41.299(2)                                    | -4.406(39)         | -3.949(37)            |
| ${}^{51}\text{Zn}$ | -9  | 359.371(44)                    | 28.796(44)                     | ${}^{51}\text{Sc}$       | -43.228(20)                                   | -3.177(60)         | -6.672(59)            |
| ${}^{28}\text{K}$  | -10 | 130.729(503)                   | 80.403(503)                    | ${}^{28}\text{F}$        | 33.115(503)                                   | -6.652(538)        | -11.300(509)          |
| ${}^{30}\text{Ca}$ | -10 | 152.958(281)                   | 73.535(281)                    | ${}^{30}\text{Ne}$       | 23.040(280)                                   | -3.149(298)        | -9.110(297)           |
| ${}^{32}\text{Sc}$ | -10 | 169.651(120)                   | 72.202(120)                    | ${}^{32}\text{Na}$       | 18.810(120)                                   | -4.705(159)        | -8.102(123)           |
| ${}^{34}\text{Ti}$ | -10 | 192.396(102)                   | 64.817(102)                    | ${}^{34}\text{Mg}$       | 8.560(90)                                     | -2.522(105)        | -7.574(105)           |
| ${}^{36}\text{V}$  | -10 | 207.654(107)                   | 64.920(107)                    | ${}^{36}\text{Al}$       | 5.950(100)                                    | -5.050(129)        | -7.572(123)           |
| ${}^{38}\text{Cr}$ | -10 | 230.442(76)                    | 57.492(76)                     | ${}^{38}\text{Si}$       | -4.170(70)                                    | -1.790(120)        | -7.313(106)           |
| ${}^{40}\text{Mn}$ | -10 | 246.974(119)                   | 56.321(119)                    | ${}^{40}\text{P}$        | -8.074(111)                                   | -4.264(147)        | -6.324(145)           |
| ${}^{42}\text{Fe}$ | -10 | 269.335(129)                   | 49.320(129)                    | ${}^{42}\text{S}$        | -17.678(124)                                  | -1.246(150)        | -5.506(175)           |
| ${}^{44}\text{Co}$ | -10 | 284.960(142)                   | 49.055(142)                    | ${}^{44}\text{Cl}$       | -20.605(137)                                  | -3.849(253)        | -5.099(207)           |
| ${}^{46}\text{Ni}$ | -10 | 306.737(56)                    | 42.638(56)                     | ${}^{46}\text{Ar}$       | -29.729(41)                                   | -0.477(65)         | -4.376(68)            |
| ${}^{48}\text{Cu}$ | -10 | 322.026(53)                    | 42.711(53)                     | ${}^{48}\text{K}$        | -32.285(2)                                    | -3.880(75)         | -5.006(74)            |
| ${}^{50}\text{Zn}$ | -10 | 342.168(29)                    | 37.928(29)                     | ${}^{50}\text{Ca}$       | -39.588(3)                                    | -2.510(39)         | -6.916(41)            |
| ${}^{31}\text{Sc}$ | -11 | 145.263(1620)                  | 88.519(1620)                   | ${}^{31}\text{Ne}$       | 30.820(1620)                                  | -7.695(1644)       | -10.844(1623)         |
| ${}^{33}\text{Ti}$ | -11 | 164.042(598)                   | 85.100(598)                    | ${}^{33}\text{Na}$       | 23.967(596)                                   | -5.609(610)        | -10.314(607)          |
| ${}^{35}\text{V}$  | -11 | 184.833(185)                   | 79.670(185)                    | ${}^{35}\text{Mg}$       | 15.640(180)                                   | -7.564(211)        | -10.085(186)          |
| ${}^{37}\text{Cr}$ | -11 | 202.764(124)                   | 77.097(124)                    | ${}^{37}\text{Al}$       | 9.810(120)                                    | -4.890(164)        | -9.940(143)           |
| ${}^{39}\text{Mn}$ | -11 | 222.689(100)                   | 72.534(100)                    | ${}^{39}\text{Si}$       | 2.320(90)                                     | -7.753(126)        | -9.543(136)           |
| ${}^{41}\text{Fe}$ | -11 | 242.261(89)                    | 68.322(89)                     | ${}^{41}\text{P}$        | -4.980(80)                                    | -4.713(149)        | -8.977(124)           |
| ${}^{43}\text{Co}$ | -11 | 261.823(105)                   | 64.121(105)                    | ${}^{43}\text{S}$        | -12.070(100)                                  | -7.512(167)        | -8.758(129)           |
| ${}^{45}\text{Ni}$ | -11 | 280.345(106)                   | 60.960(106)                    | ${}^{45}\text{Cl}$       | -18.360(100)                                  | -4.615(177)        | -8.464(235)           |
| ${}^{47}\text{Cu}$ | -11 | 299.753(97)                    | 56.912(97)                     | ${}^{47}\text{Ar}$       | -25.210(90)                                   | -6.985(112)        | -7.462(103)           |
| ${}^{49}\text{Zn}$ | -11 | 316.471(54)                    | 55.554(54)                     | ${}^{49}\text{K}$        | -29.612(3)                                    | -5.555(75)         | -9.434(76)            |

One sees that

$$\frac{\Delta B(Y=1)}{\Delta B(Y=3)} = \frac{B(A, 1) - B(A, -1)}{B(A, 3) - B(A, -3)} = \frac{1}{3}. \quad (14)$$

If the binding energies for nuclei  $B(A, 3)$ ,  $B(A, -1)$ , and  $B(A, 1)$  are available, the binding energy for unmeasured proton-rich nucleus  $B(A, -3)$  can be predicted by using

$$B(A, -3) = B(A, 3) + 3[B(A, -1) - B(A, 1)]. \quad (15)$$

Similarly, one can predict the binding energy of unknown proton-rich nucleus  $B(A, -5)$  by expressions

$$B(A, -5) = B(A, 5) + 5[B(A, -1) - B(A, 1)], \quad (16)$$

and

$$B(A, -5) = B(A, 5) + \frac{5}{3}[B(A, -3) - B(A, 3)]. \quad (17)$$

Taking the mean value for  $B(A, -5)$ , we can obtain the binding energy of  $B(A, -5)$

$$B(A, -5) = B(A, 5) + \frac{5}{2}[B(A, -1) - B(A, 1)] + \frac{5}{6}[B(A, -3) - B(A, 3)]. \quad (18)$$

Based on the isobar-mirror mass relations, the binding energy of a proton-rich odd- $A$  nucleus can be described by

$$B(A, -Y) = B(A, Y) + \sum_t \frac{2Y}{t(Y-1)} [B(A, -t) - B(A, t)] \quad (19)$$

with  $Y = 3, 5, 7, 9, \dots$  and  $t = 1, 3, 5, \dots, Y-2$ . Similarly, the binding energy for a proton-rich even- $A$  nucleus is expressed as

$$B(A, -Y) = B(A, Y) + \sum_t \frac{2Y}{t(Y-2)} [B(A, -t) - B(A, t)] \quad (20)$$

with  $Y = 4, 6, 8, 10, \dots$  and  $t = 2, 4, 6, \dots, Y-2$ .

### III. RESULTS AND DISCUSSION

#### A. Test of the ImKG mass relations

We study the binding energies of 92 pairs measured mirror nuclei based on tabulated masses (AME2011) [32], including 35 ( $Y = 1$ ), 26 ( $Y = 2$ ), 18 ( $Y = 3$ ), 12 ( $Y = 4$ ), and 1 ( $Y = 5$ ) pairs of mirror nuclei. Figure 4 shows the differences between the experimental binding energies and predicted absolute binding energies with three different theoretical models for 31 experimental measured proton-rich nuclei with  $7 \leq A \leq 41$  and  $-5 \leq Y \leq -3$ . The experimental binding energies are taken from the mass table AME2011 [32]. The solid circles are the results of the ImKG approach. The open squares and open circles denote the results of KG [31] and IM, respectively. From Fig. 4, one sees that the deviation between the ImKG calculation and the experimental data is the smallest one. We also note that for two nuclei  $^{11}\text{N}$  and  $^{14}\text{F}$ , the deviations are larger than one MeV from all three methods.

The root-mean-square (rms) deviations between the experimental binding energies [32] and model predictions

$$\sigma(M) = \left[ \frac{1}{m} \sum (B_{\text{exp}}^{(i)} - B_{\text{th}}^{(i)})^2 \right]^{1/2} \quad (21)$$

are calculated. The obtained rms deviation with respect to these 31 known masses are 0.398 MeV with ImKG mass relation, which is much smaller than the results from KG (0.502 MeV) [31] and IM (0.647 MeV) mass relations. There are  $Y(Y+1) - 1$  and  $2Y + 1$  participating nuclei involved in the ImKG predictions and in the KG mass relation, respectively. Because many more participating nuclei are involved in the ImKG predictions, the reliability for predicting the binding energies of unknown proton-rich nuclei is significantly improved.

In Table I, we list the calculated binding energies and mass excesses by using the ImKG mass relations for 144 unknown proton-rich nuclei with  $5 \leq A \leq 74$ . The estimated uncertainties are given in parentheses in keV. The uncertainty of the predicted binding energy is determined by the uncertainty of the experimental binding energies of the participating nuclei. The isotopic number  $Y = N - Z$  is listed in column 2. Columns 5 and 6 list the neutron-rich analog and the measured mass excess with its associated error in parentheses in keV.

#### B. One- and two-proton separation energies of unknown proton-rich nuclei

Based on the binding energies predicted by the ImKG mass relations, we evaluate one-proton and two-proton separation energies for proton-rich nuclei,

$$S_p(A, Z) = B(A, Z) - B(A - 1, Z - 1), \quad (22)$$

$$S_{2p}(A, Z) = B(A, Z) - B(A - 2, Z - 2). \quad (23)$$

The predicted separation energies for one-proton ( $S_p$ ) and two-proton ( $S_{2p}$ ) with the ImKG mass relations for 144 proton-rich nuclei with  $5 \leq A \leq 74$  are given in columns 7 and 8 in Table I, respectively. In the calculation, we adopt the experimental data if the mass of the nucleus is available. The masses of unknown nuclei are predicted by using the ImKG mass relations.

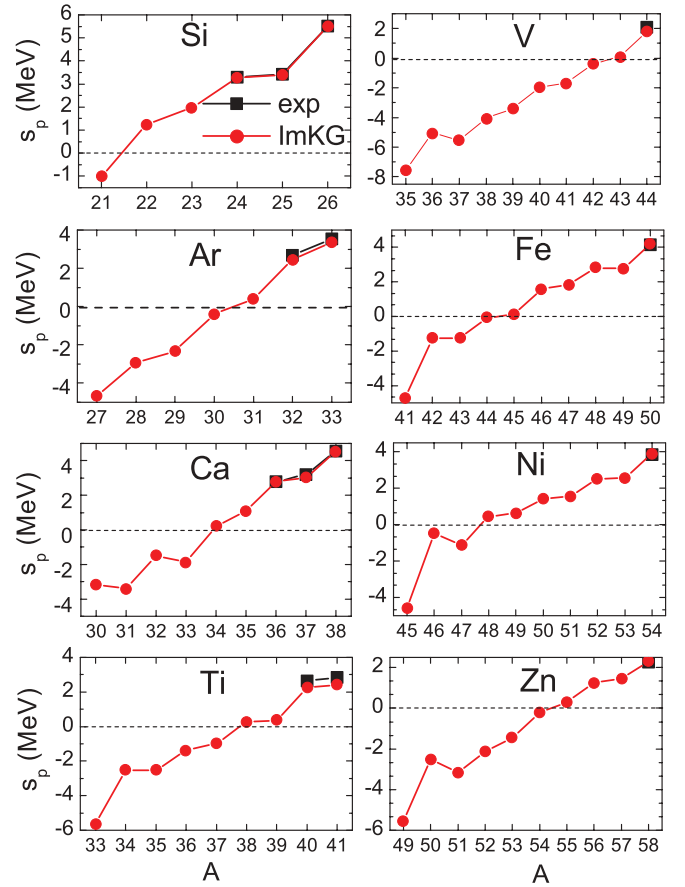


FIG. 5. (Color online) Predicted one-proton separation energies ( $S_p$  in MeV) versus mass number for proton-rich isotopes of 8 elements Si, Ar, Ca, Ti, V, Fe, Ni, and Zn, respectively.

Figures 5 and 6 show the predicted one-proton and two-proton separation energies for proton-rich isotopes of eight elements Si, Ar, Ca, Ti, V, Fe, Ni, and Zn, respectively. One sees that the odd-even staggering effect caused by the pairing interaction is evident for one-proton separation energies, and generally disappears for the two-proton separation energies.

The proton or diproton drip line is the limit beyond which nuclei become unbound (i.e.,  $S_p < 0$ , or  $S_{2p} < 0$ ) where  $S_p$  and  $S_{2p}$  are the one- and two-proton separation energy. Fourteen proton-rich nuclei beyond the proton drip line are observed in experiment, they are  $^{4,5}\text{Li}$ ,  $^{7,9}\text{B}$ ,  $^{10,11}\text{N}$ ,  $^{12}\text{O}$ ,  $^{14-16}\text{F}$ ,  $^{18,19}\text{Na}$ ,  $^{39}\text{Sc}$ , and  $^{65}\text{As}$  in Ref. [32]. Using the separation energies of nuclei listed in Table I, the positions of the proton and diproton drip lines are calculated for nuclei with  $Z = 7 - 30$ . The results are shown in Fig. 7. The solid line in black denotes the proton drip line and the solid line in red is the diproton drip line, respectively.

These nuclei with negative one-proton separation energy ( $S_p < 0$ ) and positive two-proton separation energy ( $S_{2p} > 0$ ), which lie on the left of the black line and on the right the red line, are good candidates for one-proton emissions. We list here these nuclei  $^{11}\text{N}$ ,  $^{15}\text{F}$ ,  $^{18,19}\text{Na}$ ,  $^{21}\text{Al}$ ,  $^{24-26}\text{P}$ ,  $^{30}\text{Cl}$ ,  $^{33,34}\text{K}$ ,  $^{38,39}\text{Sc}$ ,  $^{41,42}\text{V}$ ,  $^{44,45}\text{Mn}$ ,  $^{48,49}\text{Co}$ , and  $^{53-55}\text{Cu}$ . The nuclei with

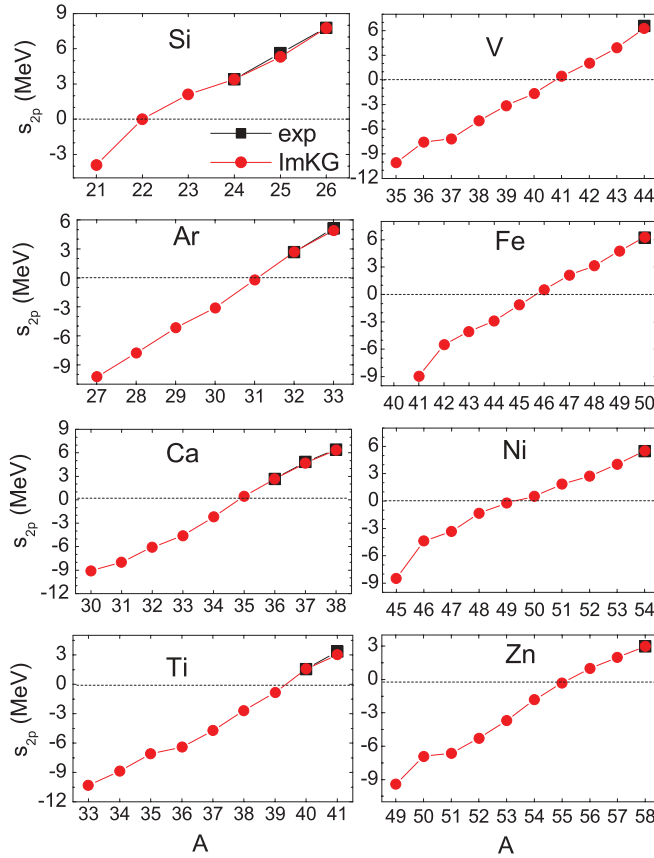


FIG. 6. (Color online) Same as Fig. 5 but for two-proton separation energies  $S_{2p}$ .

positive one-proton separation energies ( $S_p > 0$ ) and negative two-proton separation energies ( $S_{2p} < 0$ ) are good candidates for diproton emissions, which lie on the left of the red line and on the right of the black line. We list five measured proton-rich nuclei with diproton decay mode  ${}^6\text{Be}$ ,  ${}^8\text{C}$ ,  ${}^{12}\text{O}$ ,  ${}^{16}\text{Ne}$ , and  ${}^{19}\text{Mg}$ . We also list ten candidate nuclei with diproton decay mode according to the predicted masses data in Table I, they are  ${}^{22}\text{Si}$ ,  ${}^{31}\text{Ar}$ ,  ${}^{34}\text{Ca}$ ,  ${}^{38,39}\text{Ti}$ ,  ${}^{42}\text{Cr}$ ,  ${}^{45}\text{Fe}$ ,  ${}^{48,49}\text{Ni}$ , and  ${}^{55}\text{Zn}$ . We also note that if  ${}^AZ$  is a nucleus with possible proton (diproton) decay mode, then the mother nucleus  ${}^AZ + {}^4_2\text{He}$  is very often also a proton (diproton) decay nucleus. For example,  ${}^{11}\text{N}$ ,  ${}^{15}\text{F}$ , and  ${}^{19}\text{Na}$  are good candidates for one-proton emissions from the calculations, the three nuclei have the relationship  ${}^{11}\text{N} + {}^4_2\text{He} \rightarrow {}^{15}\text{F}$ ,  ${}^{15}\text{F} + {}^4_2\text{He} \rightarrow {}^{19}\text{Na}$ .

#### IV. SUMMARY

In summary, we propose a set of improved Kelson-Garvey mass relations from the mass differences of mirror nuclei including mirror nuclei far from the  $\beta$ -stability line as well as mirror nuclei near the  $N = Z$  line. The masses of 31 measured proton-rich nuclei with  $7 \leq A \leq 41$  and  $-5 \leq (N - Z) \leq -3$  can be remarkably well reproduced with the proposed method. The root-mean-square deviation is only 0.398 MeV, much smaller than the results from the traditional

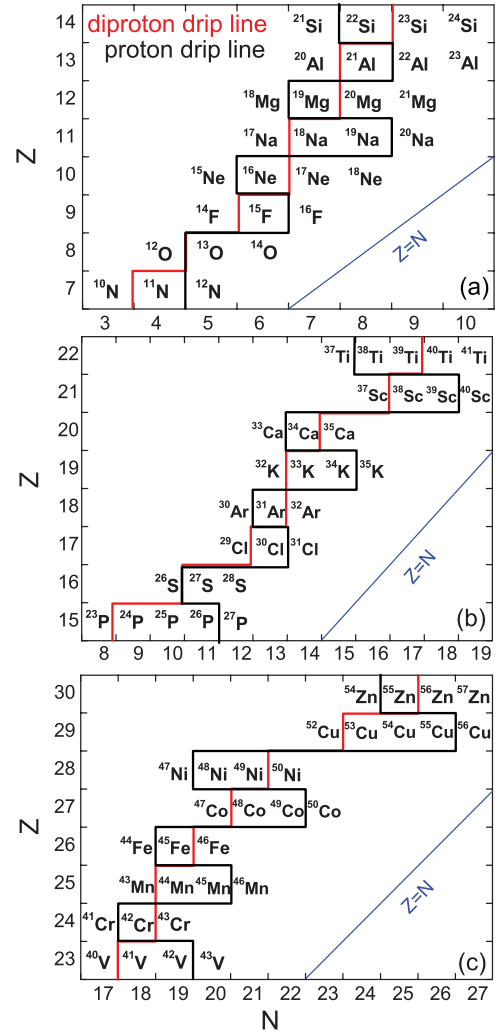


FIG. 7. (Color online) Predicted positions of proton (black line) and diproton (red line) drip lines for  $Z = 7 - 30$  with the ImKG mass relations.

Kelson-Garvey and isobar-mirror mass relations. Many more masses of participating nuclei are involved in the proposed method for the calculation of the masses of unmeasured proton-rich nuclei. We would like to emphasize that the ImKG mass relations proposed in this work are different from the extended Garvey-Kelson (GK12) mass relations proposed in Ref. [37]. The former is to predict the masses of the most proton-rich nuclei by using their neutron-rich analogs mass and the masses of participating nuclei in between, while the latter is to predict the mass of a central nucleus by using the masses of 20 neighboring nuclei around it. Binding energies and mass excesses for 144 unknown proton-rich nuclei with  $5 \leq A \leq 74$  are predicted systematically by means of the ImKG mass relations. Based on the binding energies, we have investigated the one- and two-proton separation energies, the proton drip line and the diproton drip line in the region of  $7 \leq Z \leq 30$ . The nuclei with positive one-proton separation energy but negative two-proton separation energy ( $S_p > 0$ ,  $S_{2p} < 0$ ) are good candidates for the study of diproton emissions.



## ACKNOWLEDGMENTS

This work was supported by the National Natural Science Foundation of China, Grants No. 11005003, No. 11275052,

No. 10847004, No. 11005022, and No. 10975095, and the innovation fund of undergraduate at Anyang Normal University (ASCX/2012-Z28).

- 
- [1] C. Dossat, N. Adimi, F. Aksouh *et al.*, *Nucl. Phys. A* **792**, 18 (2007).
- [2] R. Wallace and S. E. Woosley, *Astrophys. J. Suppl.* **45**, 309 (1981).
- [3] L. Van Wormer, J. Gorres, C. Iliadis *et al.*, *Astrophys. J.* **432**, 326 (1994).
- [4] C. Frohlich, G. Martinez-Pinedo, M. Liebendorfer *et al.*, *Phys. Rev. Lett.* **96**, 142502 (2006).
- [5] B. Sun, P. Zhao, and J. Meng, *Science China* **54**, 210 (2011).
- [6] H. Schatz, A. Aprahamian, J. Gorres *et al.*, *Phys. Rep.* **294**, 167 (1998).
- [7] J. Duflo and A. P. Zuker, *Phys. Rev. C* **52**, R23 (1995).
- [8] P. Moller and J. R. Nix, *At. Data Nucl. Data Tables* **59**, 185 (1995).
- [9] S. Goriely, F. Tondeur, and J. M. Pearson, *At. Data Nucl. Data Tables* **77**, 311 (2001).
- [10] S. Goriely, N. Chamel, and J. M. Pearson, *Phys. Rev. C* **82**, 035804 (2010).
- [11] L. S. Geng, H. Toki, and J. Meng, *Prog. Theor. Phys.* **113**, 785 (2005).
- [12] N. Wang, M. Liu, and X. Z. Wu, *Phys. Rev. C* **81**, 044322 (2010).
- [13] M. Liu, N. Wang, Y. G. Deng, and X. Z. Wu, *Phys. Rev. C* **84**, 014333 (2011).
- [14] N. Wang and M. Liu, *Phys. Rev. C* **84**, 051303(R) (2011).
- [15] G. Audi and A. H. Wapstra, *Nucl. Phys. A* **565**, 1 (1993).
- [16] G. Audi and A. H. Wapstra, *Nucl. Phys. A* **595**, 409 (1995).
- [17] G. Audi, A. H. Wapstra, and C. Thibault, *Nucl. Phys. A* **729**, 337 (2003).
- [18] G. T. Garvey and I. Kelson, *Phys. Rev. Lett.* **16**, 197 (1966).
- [19] J. Janecke and H. Behrens, *Phys. Rev. C* **9**, 1276 (1974).
- [20] J. E. Monahan and F. J. Serduke, *Phys. Rev. C* **15**, 1080 (1977).
- [21] J. Janecke and P. Masson, *Phys. Rev. C* **32**, 1390 (1985).
- [22] J. Barea, A. Frank, J. G. Hirsch, and P. Van Isacker, *Phys. Rev. Lett.* **94**, 102501 (2005).
- [23] J. Barea, A. Frank, J. G. Hirsch, P. Van Isacker, S. Pittel, and V. Velazquez, *Phys. Rev. C* **77**, 041304 (2008).
- [24] J. G. Hirsch, I. Morales, J. Mendoza-Temis *et al.*, *Int. J. Mod. Phys. E* **17**, 398 (2008).
- [25] I. O. Morales and A. Frank, *Phys. Rev. C* **83**, 054309 (2011).
- [26] G. J. Fu, H. Jiang, Y. M. Zhao, S. Pittel, and A. Arima, *Phys. Rev. C* **82**, 034304 (2010).
- [27] H. Jiang, G. J. Fu, Y. M. Zhao, and A. Arima, *Phys. Rev. C* **82**, 054317 (2010).
- [28] G. J. Fu, Y. Lei, H. Jiang, Y. M. Zhao, B. Sun, and A. Arima, *Phys. Rev. C* **84**, 034311 (2011).
- [29] H. Jiang, G. J. Fu, B. Sun *et al.*, *Phys. Rev. C* **85**, 054303 (2012).
- [30] I. Kelson and G. T. Garvey, *Phys. Lett.* **23**, 689 (1966).
- [31] J. Janecke and P. J. Masson, *At. Data Nucl. Data Tables* **39**, 265 (1988).
- [32] M. Wang, G. Audi, A. H. Wapstra, F. G. Kondev *et al.*, *Chin. Phys. C* **36**, 1603 (2012); <http://amdc.in2p3.fr/masstable/Ame2011int/mass.mas114>.
- [33] W. E. Ormand, *Phys. Rev. C* **55**, 2407 (1997).
- [34] S. M. Lenzi and M. A. Bentley, *Lect. Notes Phys.* **764**, 57 (2009).
- [35] S. Shlomo, *Rep. Prog. Phys.* **41**, 957 (1978).
- [36] W. E. Ormand and B. A. Brown, *Nucl. Phys. A* **491**, 1 (1989).
- [37] J. Barea, A. Frank, J. G. Hirsch *et al.*, *Eur. Phys. J. Special Topics* **150**, 189 (2007).